



1 **Building a Bimodal Landscape with Varying Bed Thicknesses in Last** 2 **Chance Canyon, New Mexico**

3 Sam Anderson¹, Nicole Gasparini¹, Joel Johnson²

4 ¹Earth and Environmental Science, Tulane University, New Orleans, 70118, USA

5 ²Jackson School of Geosciences, University of Texas at Austin, Austin, 78712, USA

6 *Correspondence to:* Sam Anderson (sanderson@tulane.edu)

7 **Abstract.** We explore how rock properties and channel morphology vary with rock type in Last Chance canyon, Guadalupe
8 mountains, New Mexico, USA. The rocks here are composed of horizontally to near horizontally interbedded carbonate and
9 sandstone. This study focuses on first and second order channel sections where the streams have a lower channel steepness
10 index (ksn) upstream and transition to a higher ksn downstream. We hypothesize that differences in bed thickness and rock
11 strength influence ksn values, both directly by influencing bulk bedrock strength but also indirectly through the production of
12 coarse sediment. We collected discontinuity intensity data (the length of bedding planes and fractures per unit area), Schmidt
13 hammer rebound measurements, and measured the largest boulder at every 40-foot elevation contour to test this hypothesis.
14 Bedrock and boulder minerology was determined using a lab-based carbonate dissolution method. High resolution
15 orthomosaics and DEMs were generated from drone photos. The orthomosaics were used to map channel sections with exposed
16 bedrock. The high-resolution DEMs were used to measure channel slope and hillslope relief. We find that discontinuity
17 intensity is negatively correlated with Schmidt hammer rebound values. Channel steepness is higher where reaches are
18 primarily incising through more thickly bedded carbonate bedrock. Where there is more thinly bedded sandstone rock exposed,
19 channel steepness tends to be lower. Furthermore, the effect that rock properties have on channel morphology is confounded
20 by sediment input from hillslopes. Thickly bedded rock units on surrounding hillslopes contribute larger sized colluvial
21 sediment to the channels, and these reaches have higher ksn. Larger and more competent carbonate sediment armors both the
22 carbonate and the more erodible sandstone and dampens the negative effect sandstone bedrock has on channel steepness. We
23 believe that in the relatively steep, high ksn downstream channel sections slope is primarily controlled by the coarse alluvial
24 cover. We further posit that the upstream low ksn reaches have a baselevel that is essentially fixed by the steep downstream
25 reaches, resulting in a stable configuration where channel slopes have adjusted to lithologic differences and/or sediment armor.

26 **1 Introduction**

27 There is little debate that rock properties impact bedrock river incision rates and channel morphology (Duvall et al., 2004;
28 Johnson et al., 2009; Harel et al., 2016). For example, Wohl et al, (1994) found that knickpoints in the Nahal Paran River,
29 Israel formed where relatively resistant chert layers were exposed. Flume experiments by Sklar and Dietrich, (2001) illustrated
30 that, all else equal, bedrock incision rate scales with the inverse square of rock tensile strength. River channels may narrow in
31 reaches with harder rocks (e.g., Bursztyn et al., 2015; Montgomery and Gran, 2001) and/or steepen (e.g., DiBiase et al, 2018;



32 Darling and Whipple, 2015). Bedrock properties can also have non-local impacts, further compounding the relationship
33 between rock properties and channel morphology. Studies have found that the abundance and calibre of sediment delivered to
34 a channel reach from upstream and/or surrounding hillslopes can steepen reaches beyond what might be predicted from channel
35 bedrock properties alone (e.g., Johnson et al., 2009; Thaler and Covington, 2016; Chilton and Spotila, 2020; Lai et al., 2021).
36 Theory suggests that in channels with the same incision rates (I) and climate, relatively less erodible rock will have a higher
37 channel steepness index (k_{sn}), or slope normalized by drainage area (Whipple and Tucker, 1999; Wobus et al., 2006). Put
38 differently,

39 Eq. (1):

$$40 I = K_c K_r k_{sn}^n, \quad (1)$$

41 where K_c and K_r are the impacts of climate and bedrock properties on erodibility, respectively, and n is a positive constant.
42 Channel steepness index can be calculated directly from a DEM, using widely available tools such as TopoToolBox
43 (Schwanghart and Scherler, 2014). Bedrock that is more resistant to fluvial erosion has a lower erodibility. Setting aside
44 challenges with estimating K_c , if there were measurable rock properties that were empirically related to K_r , we could estimate
45 bedrock incision rates without geochemical techniques or long-term field campaigns.

46 However, our community has not yet reached an empirical definition of equation 1. One challenge is that we do not know if
47 eq. 1 is universally valid. In landscapes with vertical variability in bedrock properties, numerical modelling suggests that there
48 are cases in which this relationship is inverse; in other words, less erodible rocks have a lower channel steepness index than
49 more erodible rocks (Perne et al, 2017). Even more fundamental is that there are many variables controlling rock erodibility.
50 We have a simple tool, the Schmidt Hammer, to measure relative rock compressional strength in the field. Compressional
51 strength scales directly with tensile strength (Murphy et al., 2016), which scales with incision rate (Sklar & Dietrich, 2001).
52 Unfortunately, we do not have an empirical relationship to relate Schmidt Hammer measurements to K_r . There are also
53 variables that must be measured across an area of a river reach. For example, fracture density impacts bedrock incision
54 processes (e.g., Spotila et al., 2015; Dibiase et al., 2018), but we do not know if point measurements like those obtained from
55 a Schmidt Hammer can fully quantify the impact of fracture density on erodibility. It is unlikely that a single measurement
56 tool can parameterize every bedrock property that controls incision rates. Yet, an empirical equation for estimating K_r from
57 field measurements and/or drone imagery and/or geologic maps would be extremely powerful for the tectonic geomorphology
58 community.

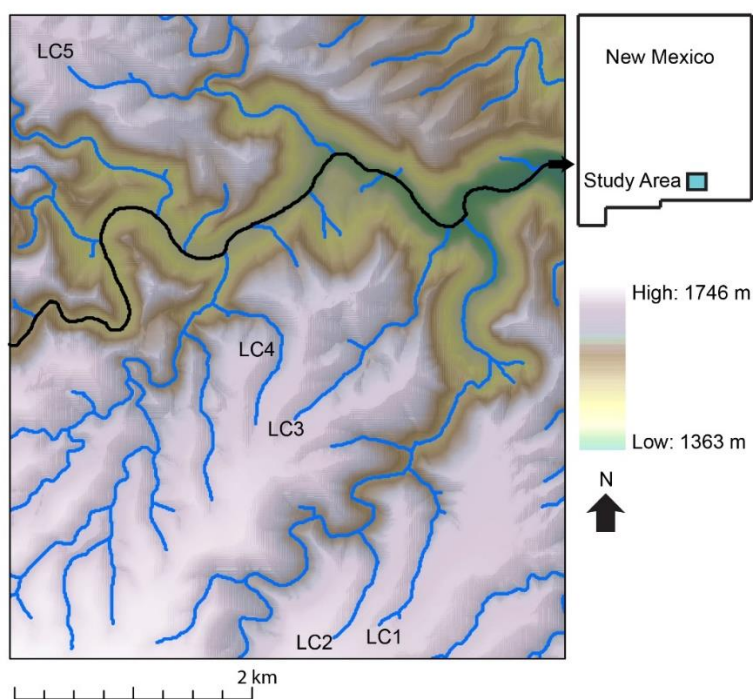
59 In this study we measure bedrock and sediment properties in first order channels in the Guadalupe Mountains, New Mexico,
60 USA. We use our measurements to inform the relationship between rock properties, erodibility, and channel morphology. Our
61 field area has alternating layers of primarily sandstone and primarily carbonite rocks. We measure some variables directly in
62 the field, such as Schmidt Hammer values of the bedrock and lengths of boulder axes. We also take advantage of imagery, to
63 calculate fracture density, and rock samples collected in the field to find rock mineralogy. We cannot develop an empirical
64 relationship for erodibility because we do not have incision rate measurements. However, we build a hypothesis for how the
65 variability in rock properties has impacted the evolution of this landscape. Our interpretation of the landscape agrees in concept



66 with numerical findings that suggest that more erodible rocks stratigraphically underlain by less erodible rocks can create a
67 scenario in which the upstream reaches of a channel have an effectively pinned baselevel even though the downstream reaches
68 are relatively steeper (Forte et al., 2016). This leads to a bimodal landscape in morphology and erodibility: higher elevation
69 topography has lower channel steepness, gentler hillslopes, and hypothesized higher erodibility; and lower elevation
70 topography has relatively high channel steepness, steeper hillslopes, and hypothesized lower erodibility.

71 2 Field Area

72 This study focuses on channels with intermittent flow in Last Chance canyon (Figure 1). During Permian time, a shallow
73 lagoon existed behind a reef complex to the south and deposited what would become interbedded carbonate and siliciclastic
74 bedrock of Last Chance Canyon (Hill, 2000; Phelps et al., 2008; Kerans et al., 2017). The Guadalupe mountains were uplifted
75 during basin and range extension beginning 27 million years ago, exposing the previously buried bedrock (Chapin and Cather,
76 1994; Ricketts et al., 2014, Hoffman, 2014; Decker et al., 2018).

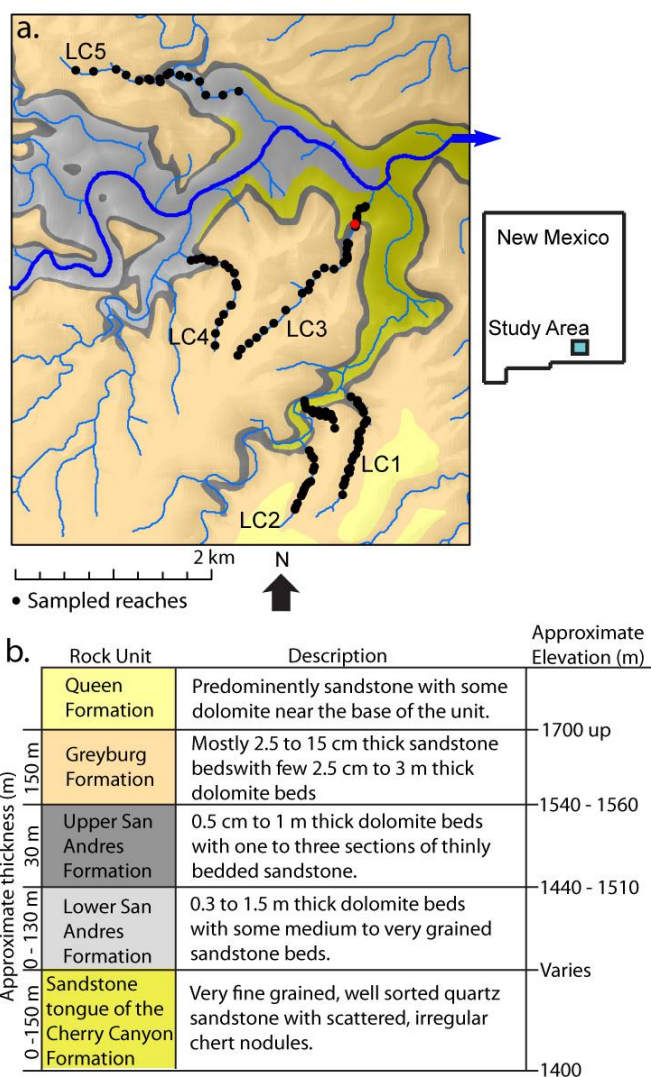


77
78 **Figure 1: Topographic map with elevations superimposed on a hillshade of Last Chance canyon with ephemeral stream channels.**
79 **Main stem of channel colored black with arrow indicating the direction of stream flow. The five channels we surveyed channels are**
80 **labeled.**

81
82 Because of its morphology and accessibility, we use data gathered within Last Chance Canyon to identify how different
83 lithologies affect stream channel and landscape morphology. Last Chance Canyon has horizontally to near horizontally bedded



84 bedrock and is currently tectonically inactive (Hill, 1987; Hill, 2006). Higher order channels further downstream in Last
 85 Chance Canyon are shallow, inundated with coarse alluvium, and have no exposed bedrock. Last Chance canyon is made up
 86 of primarily carbonate and sandstone bedrock (Scholle et al., 1992; Hill, 2000; Phelps et al., 2008). This simple variation in
 87 lithology makes Last Chance canyon an ideal location to explore the effect of varying bedrock properties on stream channel
 88 morphology. Mapped descriptions of stratigraphic units in Last Chance canyon includes both sandstone and carbonate bedrock,
 89 with thicknesses on the order of centimetres to meters (figure 2). Properties relevant to geomorphic processes at the high-
 90 resolution spatial scale required by our investigation are not included in the rock unit descriptions from published maps (NPS,
 91 2007).



92
 93 **Figure 2: a.** Geologic map of Last Chance canyon with **b.** a description of mapped lithologies (King, 1948; Boyd, 1958; Hayes, 1964;
 94 USGS, 2017). Approximate elevation and thicknesses apply only to the section of Last Chance canyon displayed here. Dots indicate



95 **locations we took measurements at (in five tributaries and one hillslope). The main stem of the channel is colored dark blue and the**
96 **arrow indicates the direction of stream flow. The five channels we surveyed are labeled LC1 through LC5. The reach marked with**
97 **a red circle is LC3.2, is shown in figure 3, and has a Lat/Long of 32.252513, -104.701289.**

98 **3 Methods**

99 **3.1 DEM Analysis**

100 We used a 10 m digital elevation model (DEM) of Last Chance canyon to determine channels of interest to survey and to
101 ascertain the location and elevation of where a channel transitions from steep to shallow channel sections (USGS, 2019). We
102 used TopoToolBox to generate longitudinal stream profiles, ksn maps, and χ (chi) plots of all surveyed channels (Schwanghart
103 and Scherler, 2014). The channel steepness index, or ksn, is a measure of channel gradient normalized for drainage area and
104 allows for the comparison of slope along a single channel or among multiple channels to isolate erosional and/or bedrock
105 erodibility patterns (Kirby & Whipple, 2012). χ , like ksn, is a way of identifying changes in channel slope along a single
106 channel or in multiple channels with varying drainage areas. Because channels can adjust to more resistant lithologic units by
107 steepening across them (Duval et al., 2004; Jansen et al., 2010), we used χ plots and ksn maps to detect changes in slope that
108 could be due to differences in bedrock erodibility and/or sediment size and cover.

109 We also used a DEM to measure channel slope and hillslope relief. Elevations were measured 75 m upstream and 75 m
110 downstream each reach, the downstream elevation was then subtracted from the upstream elevation and the value was divided
111 by the length, 150 m, to determine slope. Relief was measured in ArcGIS using a circular 500 m window around each reach.
112 500 m was chosen as the relief window because it has been shown to characterize hillslope relief (Dibiase et al., 2010).

113 **3.2 Field Survey**

114 In March and May of 2018, and in February of 2021, we surveyed five channels which we had preselected based on DEM
115 analysis, mapped geology, and accessibility. Our investigation started in lower order channels at elevations above 1400 m in
116 channels LC3, LC4, and LC5 and in elevations above 1500 in channels LC1 and LC2 (figure 1). We studied reaches of varying
117 length in the five different channels. At every ~40 ft contour interval, used for convenience and to ensure unbiased sampling,
118 we surveyed channel reaches for bedrock properties when exposed, measured the largest boulder in the reach, and took rock
119 samples from each to confirm mineralogy.

120 **3.3 Rock Properties**

121 We used a Schmidt hammer to take a minimum of 30 rebound values in each reach we surveyed that had exposed bedrock
122 (Niedzielski et al., 2009). We discarded Schmidt hammer values which were less than 10, which is the minimum value the
123 device can read, as they represent multiple values and make statistical analysis of the data difficult (Duval et al., 2004). Schmidt
124 hammer values were recorded at roughly evenly spaced intervals up the thalweg of each channel regardless of weathering or
125 presence of fractures. All Schmidt hammer values were taken perpendicular to the bedrock surface. Schmidt hammer values



126 are affected by proximal discontinuities. Because we sampled at evenly spaced intervals in the exposed bedrock and did not
127 avoid discontinuities, our Schmidt hammer values reflect a combination/distribution of local rock elastic properties modulated
128 by discontinuities (Katz et al., 2000).

129 We used a GoPro5 attached to the end of a selfie stick to take wide-angle HD videos of the bottom of 18 different reaches of
130 varying size. We used Agisoft Photoscan to generate high resolution orthomosaics of each reach using the GoPro videos and
131 then manually traced all discontinuities with Adobe Illustrator (figure 3). We placed a rock hammer of known length on the
132 bedrock surface when taking video to scale each orthomosaic to the correct length. All discontinuities by which bedrock could
133 be plucked from the thalweg were traced, including bedding planes and fractures created by weathering (Spotila, 2015). We
134 then used Fraqpac, a Matlab software suite, to determine the average discontinuity intensity, which is the average length of
135 fractures and bedding planes, per square meter, of each reach (Healy, 2017).



136

137 **Figure 3: a) An orthomosaic and b) photo of sandstone reach, LC3.2, with a discontinuity intensity of 13.03 1/m in the steep channel**
138 **section with traced discontinuities. The shadows in the orthomosaic are from the GoPro and selfie stick used to film the reach. Lat,**
139 **Long: 32.252513, -104.701289**

140 We used a drone, DJI Mavic 2 pro, to take photos of the five surveyed channels from elevations of approximately 20 meters
141 above the five stream channels, and 120 meters above adjacent hillslopes for three of the five channels. We used Agisoft
142 photoscan to generate high resolution DEMs (0.027 to 0.28 m posting) and orthomosaics of the five channels and three adjacent
143 hillslopes. We used the DEMs to take relief and slope measurements, and the orthomosaic to quantify relative proportion of
144 where stream channel beds were exposed bedrock or covered with sediment.



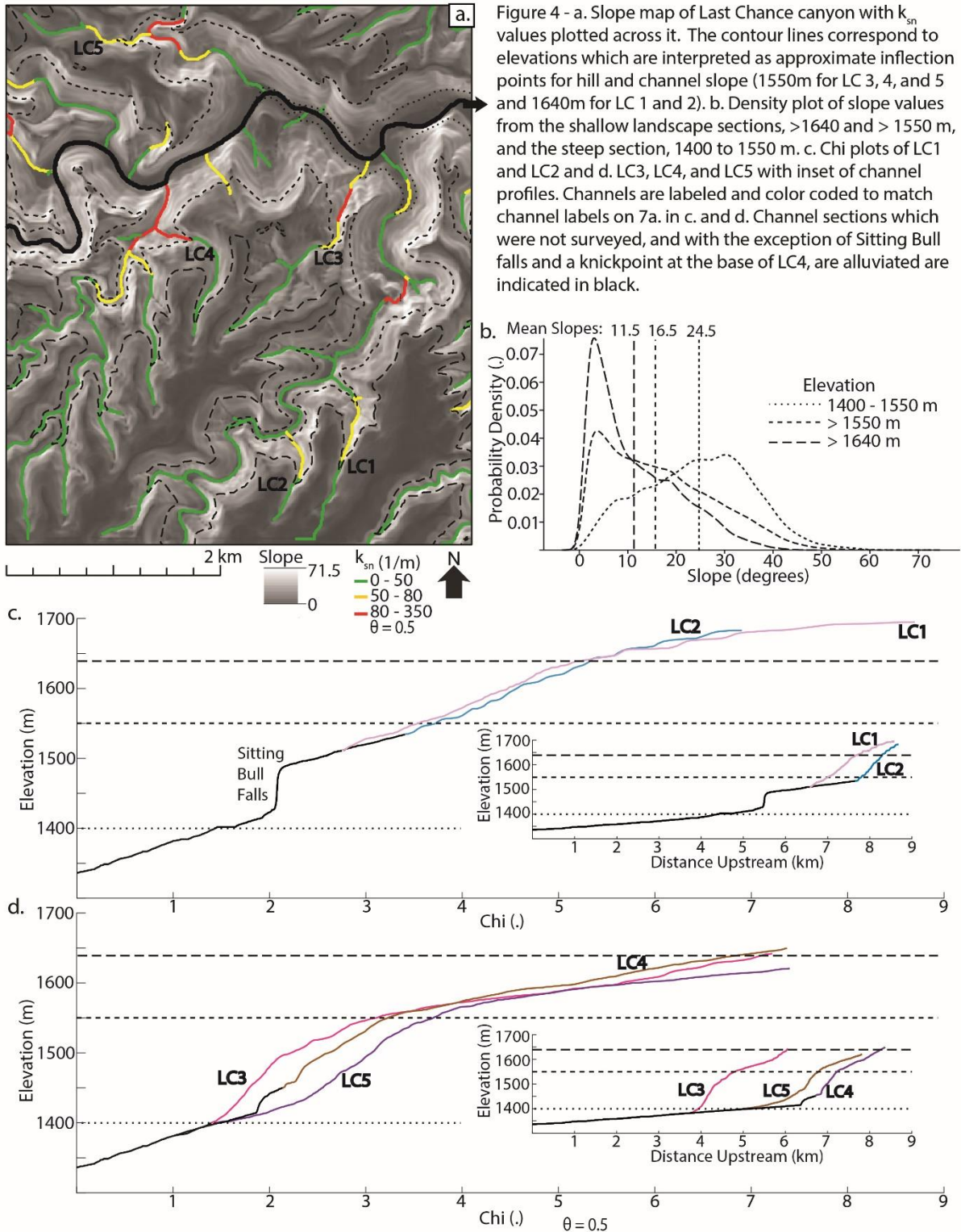
145 **3.4 Lithology**

146 At each 40 ft elevation contour interval we took rock samples from bedrock, when exposed, and from the largest boulder in
147 the stream channel to ensure correct categorization of lithology. The mineralogy of each rock sample was assumed to be
148 representative of the mineralogy of the reach or boulder it was taken from. Our efforts to determine end-member lithological
149 classifications in the field were complicated because individual samples often contained carbonate, calcite, and quartz. To find
150 a quantifiable ratio of the amount of carbonate in each sample, we ground each rock sample up using a jaw crusher and disk
151 mill. The ground up sample was rinsed in water a minimum of five times, dried in an oven over night, and then weighed the
152 following morning. We then dissolved the carbonate minerals by soaking each sample in Nitric acid for at least 24 hours. The
153 sample was again rinsed in water a minimum of five times and dried overnight. We then reweighed each sample to determine
154 the ratio amount of carbonate minerals which had dissolved. Samples were classified as carbonate if they were more than 50%
155 carbonate minerals, and sandstone rock if they were less than 60% quartz (Bell, 2005). Samples which ranged from 50 – 59%
156 of either quartz or carbonate minerals were eliminated from analysis. To ensure the validity of this methodology, we replicated
157 this processes on six of the samples and used a microscope to check that all carbonate minerals dissolved. For one of the
158 samples, we replicated this process five times. All replicate measurements demonstrated similar results (standard deviation of
159 0.62%, and variance of 0.39%), giving credence to our methodology.

160 **4 Results**

161 **4.1 Last Chance Canyon Morphology**

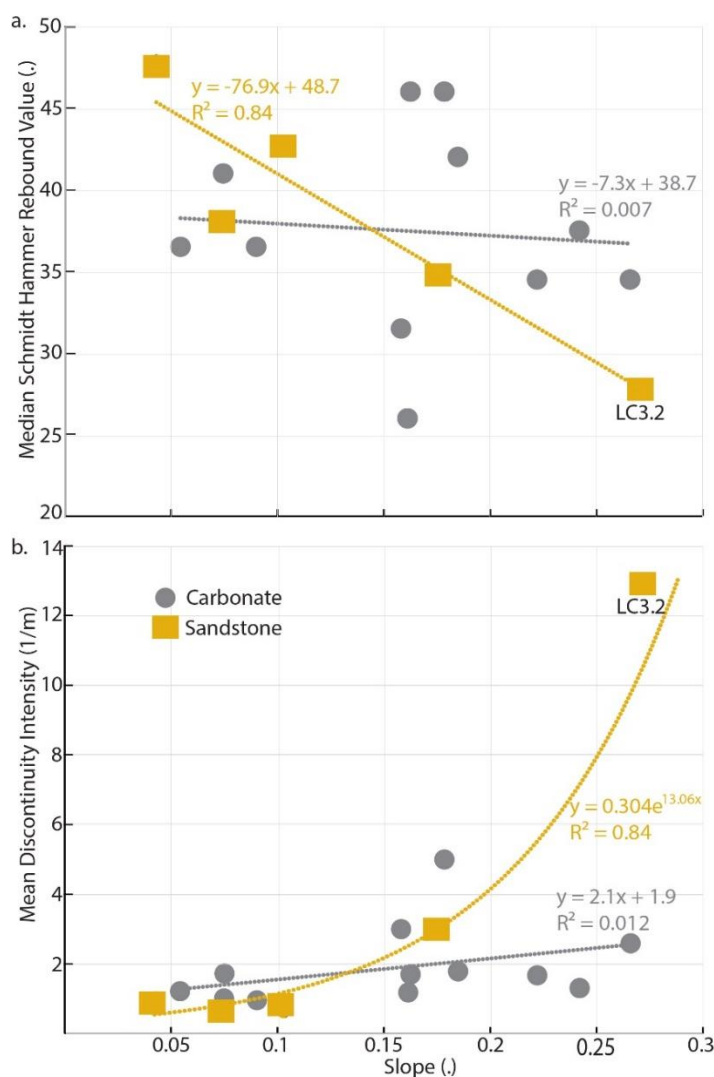
162 Last Chance canyon tributaries have upstream sections with relatively shallow channels and lower gradient hillslopes, and a
163 knickzone downstream which has steep channels and hillslopes (figure 4). Based on χ plots (figure 4c and d) and field
164 observations, we find that the stream channels transition from steep to shallow at approximately 1640 m for channels 1 and 2
165 and at approximately 1550 m for channels 3, 4 and 5. The transition from steep to shallow is more subtle in channels 1 and 2.
166 A t test verifies a bimodal distribution of hillslopes, where slope gradients above 1550 m (channels 3, 4, 5) and from above
167 1640 m (channels 1, 2) are different from hillslopes from 1400 to 1550 m.





169 **4.2 Bedrock Properties from Last Chance Canyon**

170 In Last Chance canyon, discontinuity intensity and Schmidt Hammer values change with slope in the more thinly bedded
171 sandstone rock, but not in carbonate rock (figure 5). Bedding planes are zones of weakness by which bedrock can be plucked,
172 and both bedding planes and fractures were treated as discontinuities (Spotila, 2015). Because the units are horizontally to near
173 horizontally bedded, thinly bedded sandstone rock with higher slopes have more exposed bedding planes. They also have
174 lower Schmidt hammer values (Figure 5a). However, discontinuity intensity and rebound values are invariant with slope in the
175 thickly bedded carbonate rock.



176

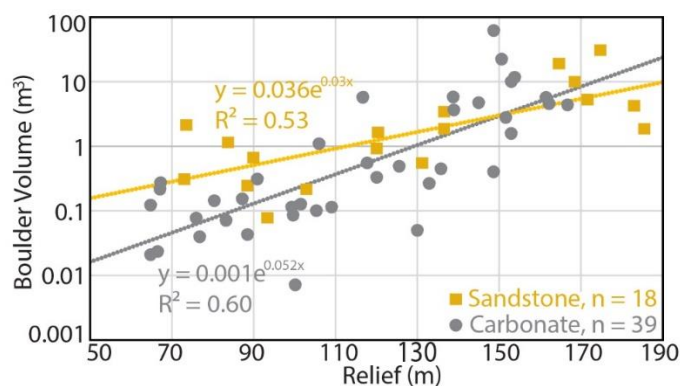
177 **Figure 5: Slope vs. a. mean Schmidt Hammer rebound value and b. mean discontinuity intensity for 5 sandstone and 11 carbonate**
178 **reaches. We calculated slope over a distance of 150 m downstream and 150 m upstream of each reach. LC3.2, which was highlighted**
179 **in figure 2 and shown in figure 3, is labeled.**



180 The average discontinuity intensity and Schmidt Hammer value from the thinly bedded sandstone in the steep channel section,
181 where more bedding planes are exposed, is 7.98 m⁻¹ (n = 2 reaches, standard deviation $\sigma = 5.04$) and 31.6 (n = 61, $\sigma = 9.5$)
182 respectively. The average discontinuity intensity of the more thickly bedded carbonate in the steep channel section is 2.34 m-
183 1 (n = 6, $\sigma = 0.56$), and they have an average Schmidt Hammer value of 36.1 (n = 240, $\sigma = 10.8$). Within the upstream channel
184 sections, the reaches have a shallower slope with fewer exposed bedding planes per channel distance. In the shallower
185 sandstone reaches, measured discontinuity intensity is smaller, 0.77 m⁻¹ (n = 3, $\sigma = 0.16$), but average Schmidt Hammer values
186 are larger, 41.7 (n = 88, $\sigma = 9.1$), in comparison with the sandstone in the steeper section. Carbonate reaches in the shallow
187 channel sections have a slightly higher discontinuity intensity of 1.51 m⁻¹ (n = 6, $\sigma = 0.32$) and average Schmidt Hammer
188 value of 37.1 (n = 90, $\sigma = 9.3$) in comparison with the shallow sandstone reaches.

189 We calculated four separate t-tests for on Schmidt hammer values from the different lithologies and channel sections in Last
190 Chance Canyon. We compared Schmidt hammer values between carbonate and sandstone reaches in the shallow and steep
191 parts of the channel and found them both to be of different populations. Schmidt hammer values for sandstone reaches in the
192 steep section were statistically different from sandstone rock in the shallow section. Schmidt hammer values for carbonate
193 reaches in steep and shallow sections were of the same statistical population. This the only test of the four in which the null
194 hypothesis was accepted and further demonstrates the lack of strong correlation between channel slope and rock strength in
195 carbonate reaches.

196 4.3 Boulder Data



197
198 **Figure 6: Relief (calculated using a 500 m window) vs. Boulder volume, calculated by multiplying the a, b, and c axis, for all boulders**
199 **we measured in the field.**

200 As relief increases the volume of the largest and most geomorphically relevant carbonate boulders increases exponentially
201 (figure 6). Relief, calculated using a 500 m window around the reach, was used to show the influence the hillslopes have in
202 contributing alluvial armor (DiBiase et al., 2010). Lower relief corresponds to the shallower upstream reaches, and the data
203 show that boulders are smaller there. In the shallow upstream channel section, there is more exposed bedrock than in stream
204 channels in the steep channel section and sediment found in the shallow reaches is generally smaller. In the steep channel



205 section, the stream channels are inundated with large sediment. The volume of sandstone boulders also increases, but less
206 dramatically than the carbonate boulders. Of the boulders we measured, 70% of the boulders in the steep section and 64% of
207 the boulders in the shallow channel section are carbonate.

208 As hillslope relief increases the length of all a, b, and c axes in carbonate boulders increases with similar slopes and with
209 relatively high r squared values (figure 7). Conversely, in sandstone boulders, the c axis correlates best with hillslope relief
210 ($R^2 = 0.54$, $m = 1.1$). the length of the b axis demonstrates a slightly weaker relationship with relief ($R^2 = 0.46$, $m = 1.8$) than
211 the c axis. The length of the a axis ($R^2 = 0.11$, $m = 0.97$) correlates poorly with relief. We choose to fit an exponential trendline
212 to the carbonate because it was a better fit. We fit a linear trendline to the sandstone because there was minimal difference
213 between the R^2 values for exponential and linear fits for the a and b axis. An exponential fit had a slightly lower R^2 value for
214 the c axis of the sandstone boulders. Carbonate boulders were slightly more equidimensional than sandstone boulders; they
215 had an average shape factor (d_{min}/d_{max}) of 0.36 ($n = 39$, $\sigma = 0.17$) while the more elongate sandstone boulders were 0.29 on
216 average ($n = 19$, $\sigma = 0.18$).

217 **5 Discussion**

218 Bedrock properties vary between lithologies and etch their signal on landscape morphology (Jansen et al., 2010; Scharf et al.,
219 2013; Bursztyn et al., 2015; Forte et al., 2016; Yanites et al., 2017). In Last Chance canyon, differences in rock properties
220 correlate with changes in channel slope and hillslope relief. Here, we introduce five key interpretations from our study. (1)
221 Discontinuity intensity affects rock strength, and channel steepness is higher where reaches are primarily within thickly bedded
222 carbonate bedrock. (2) Where more thinly bedded sandstone rock is exposed, channel steepness tends to be lower. (3)
223 Furthermore, the effect of exposed bedrock on landscape morphology is confounded by interplay with sediment input from
224 hillslopes (Duval et al., 2004; Johnson et al., 2009; Finnegan et al., 2017, Keen-Zebert et al., 2017). Thickly bedded and steeper
225 rock units on surrounding hillslopes contribute larger sized colluvial sediment to the channels, leading to steeper channel slopes
226 (Thaler and Covington, 2016). (4) Larger and more competent carbonate sediment armors both the carbonate rock and the
227 more thinly bedded sandstone and dampens the negative effect sandstone bedrock has on channel steepness. (5) We further
228 hypothesize that the landscape has adjusted to a relatively stable configuration where the shallow channel section at the top of
229 the range cuts through weaker rock and has a base level that is pinned by both the more thickly bedded rock and larger alluvium
230 in the steep downstream section.

231 A combination of local slope and bedding plane amount and spacing controls discontinuity intensity at the reach scale in
232 sandstone bedrock, but not in carbonate bedrock (figure 5). Steeper reaches cut across more horizontal bedding planes over a
233 shorter distance than shallower reaches. Thus, slope affects discontinuity intensity and rock strength differently in units with
234 less bedding planes than in more thinly bedded bedrock units. We find that thinly bedded sandstone bedrock is anisotropic,
235 where they are weaker at higher slopes and become less weak as slopes become more parallel to bedding plane orientation
236 (Weissel and Seidl, 1997). The lower slopes in sandstones develop because bulk rock properties are weaker (Bursztyn et al.,



237 2015), but when sandstone bedrock is eroded down to slopes that are sub-parallel to bedding, then their rock strength effectively
238 increases. The lack of exposed sandstone rock at higher slopes is illustrated by the single data point (LC3.2) in figure 5. We
239 posit that this one data point is an outlier, because sandstone bedrock has a higher discontinuity intensity at steeper slopes, and
240 generally is unable to sustain steep slopes in Last Chance canyon. At low slopes sandstone is more stable, as evidenced by
241 their lower discontinuity intensities and higher Schmidt hammer values (figure 5). Because carbonate bedrock is more thickly
242 bedded, its discontinuity intensity is more independent of reach scale slope than in sandstone bedrock, where discontinuity
243 intensity is very dependent on slope. Carbonate bedrock strength is not anisotropic in the same way sandstone bedrock is.
244 The landscape seemingly reflects the tendency of sandstone rock to erode to low slopes: In the shallow upstream channel
245 section, there are larger amounts of the less thickly bedded siliciclastic units exposed, while the steep channel section is mostly
246 made up of thickly bedded carbonate rock or is inundated with sediment. Sandstone reaches with higher slopes have lower
247 Schmidt hammer rebound values, because more bedding planes are exposed. Schmidt hammer values are similar between
248 carbonate reaches in the steep and shallow channel section: Our statistical analysis of Schmidt hammer values from carbonate
249 bedrock in the shallow upstream and steep downstream channel sections confirmed that they are of the same population.
250 Because the thickly bedded carbonate rock units have low discontinuity intensities regardless of slope, carbonate bedrock in
251 the shallower upstream and steeper downstream sections of Last Chance canyon have similar Schmidt hammer values,
252 suggesting that rock strength is independent of slope in carbonate bedrock.
253 The more thickly bedded and higher relief hillslopes contribute larger-sized and more geomorphically relevant boulders from
254 the hillslopes to the channel (Neely et al., 2020) (figure 6). Because siliciclastic bedrock tends to be more riddled with
255 discontinuities in the steep channel sections, we expect local shallowing. However, there are no shallow sandstone reaches in
256 the steep section. Hillslope derived sediment from the thicker bedrock armors the less thickly bedded units, dampening the
257 effect an increase in discontinuity intensity has on local shallowing (Thaler and Covington, 2016; Chilton and Spotila, 2020).
258 Within these channel sections which are inundated with sediment, we interpret that channel steepness tends to be independent
259 of bedrock properties and instead depends on the amount, size, and competency of the sediment armor. Because sandstone
260 bedrock tends to be armored by large sediment in the steep channel section there is less potential for erosion in these more
261 thinly bedded units (DiBiase et al., 2018).



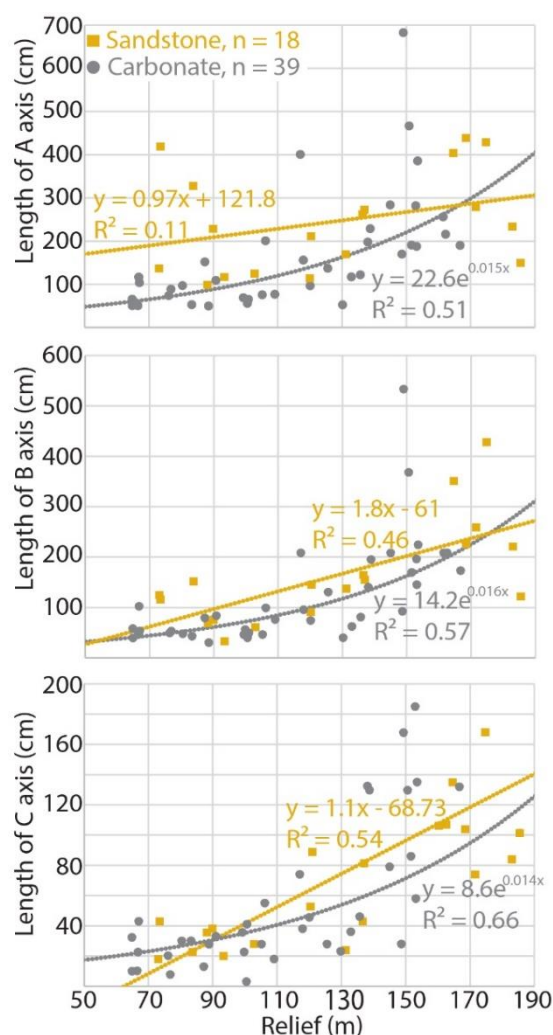
262

263 **Figure 7: Relief (calculated using a 500 m window) vs. Boulder volume, calculated by multiplying the a, b, and c axis, for all boulders**
264 **we measured in the field.**

265 Bed thickness distributions affect the shape of the large sediment measured in the channels (figure 7). Bedrock fracture patterns
266 control the initial size of sediment supplied by hillslopes (Verdian et al., 2020). Here, in Last Chance canyon, the maximum
267 length of one axis of a boulder entering a channel from proximal hillslopes is controlled by the distance between bedding
268 planes. In carbonate bedrock the distance between bedding planes tends to be longer than in sandstone bedrock. Where hillslope
269 relief increases, bedrock units are thicker, and the length of the a, b, and c axes increases for the carbonate boulders (figure 8).
270 In sandstone boulders, the c axis correlates with hillslope relief, the b axis length also correlates with relief, but to a lesser



271 extent, and the a axis length does not demonstrate any relationship with relief. Because sandstone bedrock is more thinly
272 bedded, the c axis will tend to reflect the distance between bedding planes from the source rock. The higher average shape
273 factor, 0.36, of the more equidimensional shaped carbonate boulders relative to the more rectangular dimensional sandstone
274 boulders (average shape factor, 0.29), although subtle, further speaks to the effect that the distance between bedding planes
275 affects sediment shape. Because a sediment grain tends to break across its shortest axis, the more elongate sandstone boulders
276 are generally less competent than carbonate boulders. Also, this could be why there were less sandstone than carbonate
277 boulders. Of the 58 boulders we measured, 70% in the steep channel section and 64% in the shallow were carbonate. Because
278 carbonate bedrock is thickly bedded, boulders sourced from this bedrock tend to be larger and because they are more
279 equidimensional, they likely stay larger for longer than sandstone boulders.

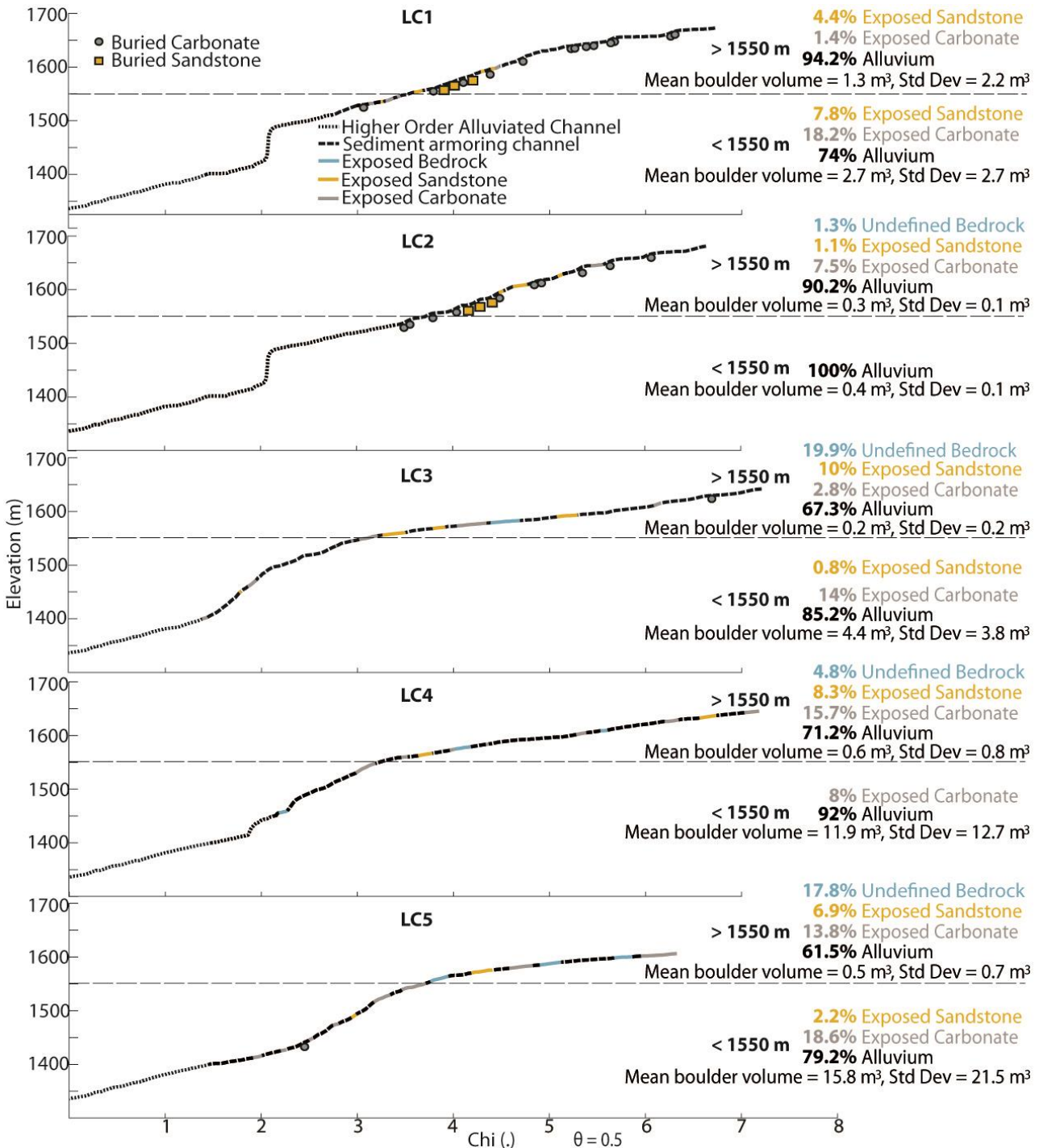


280

281 **Figure 8: Relief (calculated using a 500 m window) vs. Boulder volume, calculated by multiplying the a, b, and c axis, for all boulders**
282 **we measured in the field.**



283 The shallow channel section at the top of the range has a base level that is set by the steep, and boulder laden, channel section
284 downstream. χ plots for channels LC 3, 4, and 5, demonstrate two well defined channel sections, where in the higher elevation,
285 lower relief, and lower slope section above 1550 m there is more exposed bedrock, more exposed sandstone, less alluvium,
286 and smaller boulders armoring the channel (figure 9). Conversely, LC 1 and 2 lack the conspicuous transition from downstream
287 steep section to upstream shallow section, which is apparent in the other three channels. We hypothesize the less notable
288 change in upstream steepness in LC 1 and 2 is due to the armoring of sandstone rock units and relative abundance of alluvium
289 above 1550 m in elevation. Lithology measurements from proximal hillslopes in LC 1 and 2 indicate that just above elevation
290 1550 m there are sandstone units in the channel as in LC 3, 4, and 5 but they are buried by alluvium. By comparing LC 1 and
291 2 with 3, 4, and 5 we see how the signal from changes in rock properties is dampened by alluvium.



292

293 **Figure 9: Chi plots of LC1 - LC5 with exposed bedrock or sediment armored sections mapped. Where known, rock type is shown.**
 294 **To the left of each channel, relevant statistics for each channel are displayed from 1400 - 1550m and above 1550 m. Average boulder**
 295 **volumes, which we measured in the field, above and below 1550 m elevation are shown along with corresponding standard deviations.**



296 We hypothesize that erosion in the steep reaches of our study channels is inhibited due to an abundance of thick and resistant
297 bedrock and large immobile boulders in the steep channel section. This may seem counterintuitive, because the downstream
298 portions of our study channels are both steeper and have higher steepness indices than the upstream channel lengths (figure 4)
299 and high steepness indices are thought to correlate with high erosion rates and/or less erodible rocks (Hilley and Arrowsmith,
300 2008). Although we do not have measurements of erosion rate in Last Chance canyon, we make the link between channel
301 steepness and erodibility by assuming all channel reaches have a similar, low, erosion rate. In other parts of the Guadalupe
302 Mountains, west of Last Chance canyon, erosion rates do not depend on rock type, nor on slope (Tranel, 2020). We suggest
303 that low erodibility controls channel steepness in our study channels, and not high erosion rates. Regardless of what triggered
304 these channels to steepen or how these reaches steepened over time, given the current conditions, channel erosion is likely
305 similar in the steep and shallow landscape sections.

306 In contrast, the upstream, predominantly sandstone, channel sections also likely have minimal erosion, but for different
307 reasons. These channel reaches have lower slope and lower channel steepness indices (figure 4). Our observations of rock
308 properties and alluvial cover suggest that these upstream reaches are likely more erodible, leading to lower channel steepness.
309 Despite the lower rock strength, erosion rates may be extremely low in the upstream channel sections, because their baselevel
310 is pinned by the steep, slowly eroding downstream reaches. Such a configuration of weak, more erodible rocks that have low
311 erosion rates because of downstream, less erodible, and stable reaches has been illustrated numerically (Forte et al., 2016;
312 Perne et al., 2017). Although we do not have erosion rate measurements in our study area, numerical model predictions suggest
313 that our hypotheses are plausible. We think that any erosion in the steep portions of the channels is likely adjusted to similar
314 erosion rates in the upstream more erodible portions of the channels, leading to a relatively stable geometry. In this way, the
315 bimodal topography in Last Chance canyon has evolved to reflect the rock properties of the two dominant lithologies.

316 **6 Conclusions**

317 We present several observations about the effect of rock properties on bedrock channel steepness in Last Chance canyon. We
318 suggest that discontinuity intensity influences channel geometries. Streams steepen across sedimentary units with thicker beds
319 and lower discontinuity intensities. Conversely, channel steepness is lower in channel reaches incised into thinly bedded
320 sandstone units with higher discontinuity intensity.

321 The extent of sediment cover and the size of boulders in the channel also impacts channel morphology. More thickly bedded
322 carbonate bedrock on the hillslopes contributes larger sized, and more geomorphically relevant, alluvium to the channel. This
323 coarse carbonate sediment armors both the more and less thickly bedded bedrock and smooths channel slope across reaches
324 with different lithologies and discontinuity intensities. In Last Chance canyon, channel sections that contain larger carbonate
325 alluvium are generally steeper even if the channel bed is siliciclastic with high discontinuity intensity.

326 Finally, we hypothesize that the upstream, low channel steepness reaches draining to downstream reaches with relatively higher
327 channel steepness, create a relatively stable morphology. The more erodible shallow channel reaches at the top of the Last



328 Chance canyon have a base level that is pinned by the steep, and less erodible, channel downstream. Any erosion or lowering
329 of the steep channels will likely result in rapid lowering and smoothing of the upstream, less resistant reaches, maintaining a
330 similar channel profile through time.

331 **References**

- 332 Bell, F. G. (2005). ENGINEERING GEOLOGY| Problematic Rocks.
- 333 Bursztyn, N., Pederson, J. L., Tressler, C., Mackley, R. D., & Mitchell, K. J. (2015). Rock strength along a fluvial transect of
334 the Colorado Plateau – quantifying a fundamental control on geomorphology. *Earth and Planetary Science Letters*, 429, 90–
335 100. doi:10.1016/j.epsl.2015.07.042
- 336 Chapin, C. E., Cather, S. M., & Keller, G. R. (1994). Tectonic setting of the axial basins of the northern and central Rio Grande
337 rift. *Special Papers-Geological Society of America*, 5–5.
- 338 Chilton, K. D., & Spotila, J. A. (2020). Preservation of Valley and Ridge topography via delivery of resistant, ridge-sourced
339 boulders to hillslopes and channels, Southern Appalachian Mountains, U.S.A. *Geomorphology*, 365, 107263.
340 doi:10.1016/j.geomorph.2020.107263
- 341 Darling, A., & Whipple, K. (08 2015). Geomorphic constraints on the age of the western Grand Canyon. *Geosphere*, 11(4),
342 958–976. doi:10.1130/GES01131.1
- 343 Decker, D. D., Polyak, V. J., Asmerom, Y., & Lachniet, M. S. (2018). U--Pb dating of cave spar: a new shallow crust landscape
344 evolution tool. *Tectonics*, 37(1), 208–223.
- 345 DiBiase, R. A., Rossi, M. W., & Neely, A. B. (2018). Fracture density and grain size controls on the relief structure of bedrock
346 landscapes. *Geology*, 46(5), 399–402. doi:10.1130/G40006.1
- 347 DiBiase, R. A., Whipple, K. X., Heimsath, A. M., & Ouimet, W. B. (2010). Landscape form and millennial erosion rates in
348 the San Gabriel Mountains, CA. *Earth and Planetary Science Letters*, 289(1), 134–144. doi:10.1016/j.epsl.2009.10.03
- 349 Duvall, A., Kirby, E., & Burbank, D. (2004). Tectonic and lithologic controls on bedrock channel profiles and processes in
350 coastal California. *Journal of Geophysical Research: Earth Surface*, 109(F3). doi:10.1029/2003JF000086
- 351 Forte, A. M., Yanites, B. J., & Whipple, K. X. (2016). Complexities of landscape evolution during incision through layered
352 stratigraphy with contrasts in rock strength. *Earth Surface Processes and Landforms*, 41(12), 1736–1757. doi:10.1002/esp.3947
- 353 Finnegan, N. J., Klier, R. A., Johnstone, S., Pfeiffer, A. M., & Johnson, K. (2017). Field evidence for the control of grain size
354 and sediment supply on steady-state bedrock river channel slopes in a tectonically active setting. *Earth Surface Processes and*
355 *Landforms*, 42(14), 2338–2349.
- 356 Harel, M.-A., Mudd, S. M., & Attal, M. (2016). Global analysis of the stream power law parameters based on worldwide ¹⁰Be
357 denudation rates. *Geomorphology*, 268, 184–196. doi:10.1016/j.geomorph.2016.05.035
- 358 Healy, D., Rizzo, R. E., Cornwell, D. G., Farrell, N. J. C., Watkins, H., Timms, N. E., ... Smith, M. (2017). FracPaQ: A
359 MATLAB toolbox for the quantification of fracture patterns. *Journal of Structural Geology*, 95, 1–16.



- 360 Hill, C. A. (1987). Geology of Carlsbad cavern and other caves in the Guadalupe Mountains, New Mexico and Texas. Bull.
361 117, New Mexico Bureau of Mines and Minerals Resources.
- 362 Hill, C. A., & Others. (2000). Overview of the geologic history of cave development in the Guadalupe Mountains, New
363 Mexico. *Journal of Cave and Karst Studies*, 62(2), 60–71.
- 364 Hill, C. A. (2006). Geology of the Guadalupe Mountains: An overview of recent ideas. *Caves and karst of southeastern New*
365 *Mexico: Guidebook, 57th Field Conference*, New Mexico Geological Society, Guidebook, 57th Field Conference, 145–150.
- 366 Hilley, G. E., & Arrowsmith, J. R. (2008). Geomorphic response to uplift along the Dragon’s Back pressure ridge, Carrizo
367 Plain, California. *Geology*, 36(5), 367–370.
- 368 Hoffman, L. L. (2014). Spatial variability of erosion patterns along the eastern margin of the Rio Grande Rift. Illinois State
369 University.
- 370 Jansen, J. D., Codilean, A. T., Bishop, P., & Hoey, T. B. (2010). Scale dependence of lithological control on topography:
371 Bedrock channel geometry and catchment morphometry in western Scotland. *The Journal of geology*, 118(3), 223–246.
- 372 Johnson, J. P. L., Whipple, K. X., Sklar, L. S., & Hanks, T. C. (2009). Transport slopes, sediment cover, and bedrock channel
373 incision in the Henry Mountains, Utah. *Journal of Geophysical Research: Earth Surface*, 114(F2). doi:10.1029/2007JF000862
- 374 Katz, O., Reches, Z., & Roegiers, J.-C. (2000). Evaluation of mechanical rock properties using a Schmidt Hammer.
375 *International Journal of rock mechanics and mining sciences*, 37(4), 723–728.
- 376 Keen-Zebert, A., Hudson, M. R., Shepherd, S. L., & Thaler, E. A. (2017). The effect of lithology on valley width, terrace
377 distribution, and bedload provenance in a tectonically stable catchment with flat-lying stratigraphy. *Earth Surface Processes*
378 *and Landforms*, 42(10), 1573–1587.
- 379 Kerans, C., Zahm, C., Garcia-Fresca, B., & Harris, P. M. (2017). Guadalupe Mountains, West Texas and New Mexico: Key
380 excursions. *AAPG Bulletin*, 101(4), 465–474.
- 381 Kirby, E., & Whipple, K. X. (2012). Expression of active tectonics in erosional landscapes. *Journal of structural geology*, 44,
382 54–75.
- 383 Konare, A., Zakey, A. S., Solmon, F., Giorgi, F., Rauscher, S., Ibrah, S., & Bi, X. (2008). A regional climate modeling study
384 of the effect of desert dust on the West African monsoon. *Journal of Geophysical Research: Atmospheres*, 113(D12).
- 385 Lai, L. S.-H., Roering, J. J., Finnegan, N. J., Dorsey, R. J., & Yen, J.-Y. (2021). Coarse sediment supply sets the slope of
386 bedrock channels in rapidly uplifting terrain: Field and topographic evidence from eastern Taiwan. *Earth Surface Processes*
387 *and Landforms*, 46(13), 2671–2689. doi:10.1002/esp.5200
- 388 Montgomery, D. R., & Gran, K. B. (2001). Downstream variations in the width of bedrock channels. *Water Resources*
389 *Research*, 37(6), 1841–1846. doi:10.1029/2000WR900393
- 390 Murphy, B., Johnson, J., Gasparini, N., & Sklar, L. (04 2016). Chemical weathering as a mechanism for the climatic control
391 of bedrock river incision. *Nature*, 532, 223–227. doi:10.1038/nature17449
- 392 National Park Service Resources Inventory Program Lakewood Colorado, (2007). Digital geologic map of Guadalupe
393 Mountains National Park and vicinity, Texas (NPS, GRD, GRE, GUMO).



- 394 Niedzielski, T., Migoń, P., & Placek, A. (2009). A minimum sample size required from Schmidt hammer measurements. *Earth*
395 *Surface Processes and Landforms: The Journal of the British Geomorphological Research Group*, 34(13), 1713–1725.
- 396 Perne, M., Covington, M. D., Thaler, E. A., & Myre, J. M. (2017). Steady state, erosional continuity, and the topography of
397 landscapes developed in layered rocks. *Earth Surface Dynamics*, 5(1), 85–100. doi:10.5194/esurf-5-85-2017
- 398 Phelps, R. M., Kerans, C., Scott, S. Z., Janson, X., & Bellian, J. A. (2008). Three-dimensional modelling and sequence
399 stratigraphy of a carbonate ramp-to-shelf transition, Permian Upper San Andres Formation. *Sedimentology*, 55(6), 1777–1813.
- 400 Ricketts, J. W., Karlstrom, K. E., Priewisch, A., Crossey, L. J., Polyak, V. J., & Asmerom, Y. (2014). Quaternary extension in
401 the Rio Grande rift at elevated strain rates recorded in travertine deposits, central New Mexico. *Lithosphere*, 6(1), 3–16.
- 402 Scharf, T. E., Codilean, A. T., De Wit, M., Jansen, J. D., & Kubik, P. W. (2013). Strong rocks sustain ancient postorogenic
403 topography in southern Africa. *Geology*, 41(3), 331–334.
- 404 Scholle, P. A., Ulmer, D. S., & Melim, L. A. (1992). Late-stage calcites in the Permian Capitan Formation and its equivalents,
405 Delaware Basin margin, west Texas and New Mexico: evidence for replacement of precursor evaporites. *Sedimentology*,
406 39(2), 207–234.
- 407 Schwanghart, W., & Scherler, D. (2014). Short Communication: TopoToolbox 2 – MATLAB-based software for topographic
408 analysis and modeling in Earth surface sciences. *Earth Surface Dynamics*, 2(1), 1–7. doi:10.5194/esurf-2-1-2014
- 409 Sklar, L. S., & Dietrich, W. E. (12 2001). Sediment and rock strength controls on river incision into bedrock. *Geology*, 29(12),
410 1087–1090. doi:10.1130/0091-7613(2001)029<1087:SARSCO>2.0.CO;2
- 411 Spotila, J. A., Moskey, K. A., & Prince, P. S. (2015). Geologic controls on bedrock channel width in large, slowly-eroding
412 catchments: Case study of the New River in eastern North America. *Geomorphology*, 230, 51–63.
413 doi:10.1016/j.geomorph.2014.11.004
- 414 Thaler, E. A., & Covington, M. D. (2016). The influence of sandstone caprock material on bedrock channel steepness within
415 a tectonically passive setting: Buffalo National River Basin, Arkansas, USA. *Journal of Geophysical Research: Earth Surface*,
416 121(9), 1635–1650. doi:10.1002/2015JF003771
- 417 Tranel, L. M., & Happel, A. A. (2020). Evaluating escarpment evolution and bedrock erosion rates in the western Guadalupe
418 Mountains, West Texas and New Mexico. *Geomorphology*, 368, 107335.
- 419 US Geologic Survey, 2017, 1/3rd arc-second digital elevation models (DEMs). USGS National Map 3DEP downloadable data
420 collection.
- 421 Verdian, J. P., Sklar, L. S., Riebe, C. S., & Moore, J. R. (2021). Sediment size on talus slopes correlates with fracture spacing
422 on bedrock cliffs: implications for predicting initial sediment size distributions on hillslopes. *Earth Surface Dynamics*, 9(4),
423 1073–1090.
- 424 Whipple, K. X., & Tucker, G. E. (1999). Dynamics of the stream-power river incision model: Implications for height limits of
425 mountain ranges, landscape response timescales, and research needs. *Journal of Geophysical Research: Solid Earth*, 104(B8),
426 17661–17674. doi:10.1029/1999JB900120



- 427 Wobus, C., Whipple, K. X., Kirby, E., Snyder, N., Johnson, J., Spyropolou, K., ... Sheehan, D. (01 2006). Tectonics from
428 topography: Procedures, promise, and pitfalls. *Tectonics, Climate, and Landscape Evolution*. doi:10.1130/2006.2398(04)
- 429 Wohl, E. E., Greenbaum, N., Schick, A. P., & Baker, V. R. (1994). Controls on bedrock channel incision along nahal paran,
430 Israel. *Earth Surface Processes and Landforms*, 19(1), 1–13. doi:10.1002/esp.3290190102
- 431 Yanites, B. J., Becker, J. K., Madritsch, H., Schnellmann, M., & Ehlers, T. A. (2017). Lithologic effects on landscape response
432 to base level changes: a modeling study in the context of the Eastern Jura Mountains, Switzerland. *Journal of Geophysical*
433 *Research: Earth Surface*, 122(11), 2196–2222.
- 434 Yanites, B. J. (2018). The dynamics of channel slope, width, and sediment in actively eroding bedrock river systems. *Journal*
435 *of Geophysical Research: Earth Surface*, 123(7), 1504–1527.
- 436 Zaleski, E., Eaton, D. W., Milkereit, B., Roberts, B., Salisbury, M., & Petrie, L. (1997). Seismic reflections from subvertical
437 diabase dikes in an Archean terrane. *Geology*, 25(8), 707–710.